Theoretical Studies of Organometallic Compounds. 6. Structures and Bond Energies of $M(CO)_n^+$, MCN, and $M(CN)_2^-$ (M = Ag, Au; n = 1–3)[1]

Achim Veldkamp and Gernot Frenking*

Fachbereich Chemie, Philipps-Universität Marburg, Hans-Meerwein-Strasse, D-3550 Marburg, Germany

Received August 16, 1993®

Quantum mechanical ab initio calculations using relativistic effective core potentials for the metals are employed to predict theoretically the geometries, vibrational spectra, and metal–ligand bond energies of the title compounds. The comparison with available experimental data shows very good agreement. The dicarbonyls $Ag(CO)_2^+$ and $Au(CO)_2^+$ are predicted to be more stable than the mono- and tricarbonyls, respectively. The Au(I) complexes are stronger bound than the Ag(I) complexes, and the cyanides have much stronger metal–ligand bonds than the carbonyls. The topological analysis of the electronic structures and the natural bond orbital analysis show that the origin of the metal–ligand bonds in the carbonyls and cyanides is dominantly electrostatic, but covalent contributions are analyzed for $Ag(CO)_2^+$, $AuCO^+$, $Au(CO)_2^+$, and the nitriles $M(CN)_2$. The covalent contribution to the metal–ligand bond increases from MCO^+ to $M(CO)_2^+$, but it decreases strongly from $M(CO)_2^+$ to $M(CO)_3^+$. The covalent character of the M–C bonds arises from σ donation of the ligand with negligible π back-donation, which agrees with the calculated and observed frequency shift toward higher wavenumbers for the C–O and C–N stretching modes.

1. Introduction

To the large class of transition metal carbonyl complexes[2] some intriguing Ag(I) and Au(I) complexes with unusual properties have recently been added. Hurlburt et al.[3] reported the synthesis and X-ray structure analysis of $[Ag(CO)][B(OTeF_5)_4]$, the first isolable silver carbonyl complex. The same group has now succeeded in isolating and crystallizing the thermally very labile complex $[Ag(CO)_2][B(OTeF_5)_4]$.[4] The X-ray structure analysis of this compound is the first example of a $M(CO)_2^+$ complex. At the same time, Willner et al.[5] reported the synthesis and vibrational spectrum of the first thermally stable $Au(CO)_2^+$ complex, i.e. $[Au(CO)_2][Sb_2F_{11}]$. A remarkable feature of these carbonyl complexes is the finding that the CO stretching frequency ν_{CO} is significantly shifted toward *higher* wavenumbers relative to CO, whereas most other metal carbonyls exhibit *lower* stretching frequencies ν_{CO}.[1,5] Also the force constant for the CO stretching mode f_{CO} is clearly higher in $M(CO)_n^+$ (M = Ag, Au; n = 1, 2) carbonyls than in CO.[5] The highest frequency was found in solid $[Au(CO)_2][Sb_2F_{11}]$ with $\nu_{CO,asym}$ = 2254 cm^{-1}, which is more than 100 cm^{-1} higher than that in CO (2143 cm^{-1}).[5] The X-ray analyses of $[Ag(CO)][B(OTeF_5)_4]$[3] and $[Ag(CO)_2][B(OTeF_5)_4]$[4] indicate shorter C–O bond distances than in CO, which is in agreement with the frequency shift.

The increase in the stretching frequency ν_{CO} in the silver and gold carbonyls $M(CO)_n^+$ was explained by negligible π back-donation of the metal to the CO π^* orbital, which means that CO acts as a pure Lewis base.[3,5] Because the carbon lone-pair HOMO in CO is slightly antibonding,[6] electron donation from CO yields a stronger and shorter bond. This is the reason that CO^+ and HCO^+ have shorter C–O bonds and higher stretching frequencies ν_{CO} than CO.[7]

In order to gain insight into the unusual features of the M–C bonds and to explain the experimentally observed[3–5] intriguing properties of the metal carbonyls MCO^+ and $M(CO)_2^+$ (M = Ag, Au), we performed ab initio calculations on the geometries, vibrational frequencies, M–CO bond energies, and electronic structures of $AgCO^+$ (1), $Ag(CO)_2^+$ (2), $Ag(CO)_3^+$ (3), $AuCO^+$ (4), $Au(CO)_2^+$ (5), and $Au(CO)_3^+$ (6). We also studied theoretically the isoelectronic cyano complexes AgCN (7), $Ag(CN)_2^-$ (8), AuCN (9), and $Au(CN)_2^-$ (10). Relativistic effective core potentials (ECP)[8] are used for the metals and all electron wave functions are employed for the other atoms. The electronic structure is investigated using the natural bond orbital (NBO) partitioning scheme developed by Weinhold and co-workers[9] and the topological analysis of the electron density distribution and its associated Laplacian developed by Bader and co-workers.[10]

• Abstract published in *Advance ACS Abstracts*, October 15, 1993.

(1) Part V: Neuhaus, A.; Stegmann, R.; Frenking, G. *J. Am. Chem. Soc.*, in press.

(2) Werner, H. *Angew. Chem.* **1990**, *102*, 1109; *Angew. Chem., Int. Ed. Engl.* **1990**, *29*, 1077.

(3) Hurlburt, P. K.; Anderson, O. P.; Strauss, S. H. *J. Am. Chem. Soc.* **1991**, *113*, 6277.

(4) Hurlburt, P. K.; Rack, J. J.; Dec, S. F.; Anderson, O. P.; Strauss, S. H. *Angew. Chem.*, in press.

(5) Willner, H.; Schaebs, J.; Hwang, G.; Mistry, F.; Jones, R.; Trotter, J.; Aubke, F. *J. Am. Chem. Soc.* **1992**, *114*, 8972.

(6) (a) D'Amico, K. L.; Trenary, M.; Shinn, N. D.; Solomon, E. I.; McFeely, F. R. *J. Am. Chem. Soc.* **1982**, *104*, 5102. (b) Tevault, D.; Nakamoto, K. *Inorg. Chem.* **1976**, *15*, 1282. (c) DeKock, R. L.; Sarapu, A. C.; Fenske, R. F. *Inorg. Chem.* **1971**, *10*, 38.

(7) (a) Herzberg, G. *Spectra of Diatomic Molecules*, 2nd. ed.; Van Nostrand: New York, 1950. (b) Hirota, E.; Endo, J. *J. Mol. Spectrosc.* **1988**, *127*, 524.

(8) Hay, P. J.; Wadt, W. R. *J. Chem. Phys.* **1985**, *82*, 299.

(9) (a) Reed, A. E.; Curtiss, L. A.; Weinhold, F. *Chem. Rev.* **1988**, *88*, 899. (b) Weinhold, F.; Carpenter, J. E. In *The Structure of Small Molecules and Ions*; Naaman, R., Vager, Z., Eds.; Plenum: New York, 1988; p 227.

(10) (a) Bader, R. F. W.; Tal, Y.; Anderson, S. G.; Nguyen-Dang, T. T. *Isr. J. Chem.* **1980**, *19*, 8. (b) Bader, R. F. W.; Nguyen-Dang, T. T.; Tal, Y. *Rep. Prog. Phys.* **1981**, *44*, 893. (c) Bader, R. F. W.; Nguyen-Dang, T. T. *Adv. Quantum Chem.* **1981**, *14*, 63. (d) Bader, R. F. W. *Atoms in Molecules. A Quantum Theory*; Oxford Press: Oxford, U.K., 1990.

0276-7333/93/2312-4613$04.00/0

Table I. Optimized Bond Distances r_{A-B} (Å) and Total Energies (hartrees) for Structures 1–10, CO, and CN^- at MP2/I (Results Calculated at HF/I in Parentheses)

						exp	
molecule	symm	state	E_{tot}	r_{M-C}	r_{C-X}	r_{M-C}	r_{C-X}
$AgCO^+$ (1)	$C_{\infty v}$	$^1\Sigma^+$	−257.8115	2.329	1.143	2.10[a]	1.077[a]
			(−257.4156)	(2.511)	(1.103)		
$Ag(CO)_2^+$ (2)	$D_{\infty h}$	$^1\Sigma_g^+$	−370.8687	2.216	1.143	2.06–2.20[b]	1.07–1.09[b]
			(−370.1729)	(2.440)	(1.103)		
$Ag(CO)_3^+$ (3)	D_{3h}	$^1A_1'$	−483.9052	2.322	1.144		
			(−482.9227)	(2.554)	(1.104)		
$AuCO^+$ (4)	$C_{\infty v}$	$^1\Sigma^+$	−247.3888	1.975	1.143		
			(−247.0161)	(2.145)	(1.099)		
$Au(CO)_2^+$ (5)	$D_{\infty h}$	$^1\Sigma_g^+$	−360.4828	2.009	1.142	2.05[g]	1.11[g]
			(−359.7996)	(2.089)	(1.099)		
$Au(CO)_3^+$ (6)	D_{3h}	$^1A_1'$	−473.5130	2.096	1.145		
			(−472.5347)	(2.281)	(1.102)		
AgCN (7)	$C_{\infty v}$	$^1\Sigma^+$	−237.5987	2.087	1.188		
			(−237.1936)	(2.152)	(1.145)		
$Ag(CN)_2^-$ (8)	$D_{\infty h}$	$^1\Sigma_g^+$	−330.3084	2.090	1.190	2.01–2.07[c]	1.13–1.14[c]
			(−329.6031)	(2.165)	(1.148)		
AuCN (9)	$C_{\infty v}$	$^1\Sigma^+$	−227.2138	1.929	1.187		
			(−226.8310)	(1.996)	(1.141)		
$Au(CN)_2^-$ (10)	$D_{\infty h}$	$^1\Sigma_g^+$	−319.9570	2.005	1.189	1.91–2.06[d]	1.12–1.18[d]
			(−319.2733)	(2.052)	(1.146)		
CO	$C_{\infty v}$	$^1\Sigma^+$	−113.0166		1.152		1.128[e]
			(−112.7373)		(1.114)		
CN^-	$C_{\infty v}$	$^1\Sigma^+$	−92.5583		1.202		1.154[f]
			(−92.2849)		(1.160)		

[a] Reference 3. [b] Reference 4. [c] References 27 and 28. [d] Reference 29. [e] Reference 79. [f] Reference 34. [g] Estimated values, ref 5.

There are very few ab initio studies of the molecular ions **1–10**. $AgCO^+$ (**1**) and $Ag(CO)_2^+$ (**2**) have been investigated in a comparative study of first- and second-row transition metal carbonyl ions by Barnes et al.[11] Theoretical studies of the corresponding gold complexes $AuCO^+$ (**4**) and $Au(CO)_2^+$ (**5**) and the tricarbonyl ions $Ag(CO)_3^+$ (**3**) and $Au(CO)_3^+$ (**6**) are not known to us. Sano et al.[12] reported Xα calculations for $Ag(CN)_2^-$ (**8**) and $Au(CN)_2^-$ (**10**). The gold cyano complexes **9** and **10** were the subject of a theoretical study by Schwerdtfeger et al.[13] Ab initio calculations on AgCN (**7**) have not so far been published.

2. Theoretical Details

The geometry optimizations were performed at the Hartree–Fock and MP2[14] level of theory. For Ag and Au, the quasi-relativistic ECP developed by Hay and Wadt[8] with a split valence basis set [441/2111/31] for Ag and [441/2111/21] for Au and the all-electron 6-31G(d) basis set[15] for the other atoms was used. The ECP for Ag and Au incorporates the mass–velocity and Darwin relativistic terms into the potential.[8] This basis set is denoted I. Systematic studies have shown[1,16] that the geometries of closed-shell transition metal complexes are predicted at this level of theory in good agreement with experiment. The vibrational frequencies and zero-point energies ZPE are calculated at MP2/I.

Improved total energies have been calculated using Møller–Plesset perturbation theory[14] terminated at fourth order (MP4(SDQ)) and at the quadratic CI level with an estimate of the triple substitutions QCISD(T).[17] For the MP4 and QCISD(T) calculations the less contracted ECP[8] valence basis sets augmented by a set of additional f-type polarization functions[18] [3311/2111/211/1] for Ag and [3311/2111/111/1] for Au and the 6-31G(d) basis set for the other atoms are employed. The exponents for the set of f-type polarization functions are 1.611 for Ag and 1.050 for Au.[18] These levels of theory are denoted MP4/II and QCISD(T). The calculations have been carried out using the Convex version of Gaussian 92.[19]

Unless otherwise noted, geometries discussed in this paper were optimized at MP2/I, and calculated energies, at QCISD(T)/II//MP2/I.

For the calculation of the electron density distribution $\rho(\mathbf{r})$, the gradient vector field $\nabla\rho(\mathbf{r})$, and its associated Laplacian $\nabla^2\rho(\mathbf{r})$ the programs PROAIM, SADDLE, GRID, and GRDVEC were used.[20] The NBO analysis[9] was carried out using Gaussian 92.[19]

3. Results and Discussion

Table I shows the theoretically predicted geometries of the cations **1–10** in comparison with experimental results. Table II shows the theoretical and experimental vibrational frequencies. The calculated dissociation energies D_e are displayed in Table III.

(11) Barnes, L. A.; Rosi, M.; Bauschlicher, C. W. *J. Chem. Phys.* **1990**, *93*, 609.
(12) (a) Sano, M.; Yamatera, H. *Bull. Chem. Soc. Jap.* **1981**, *54*, 2023. (b) Sano, M.; Adachi, H.; Yamatera, H. *Bull. Chem. Soc. Jap.* **1982**, *55*, 1022.
(13) Schwerdtfeger, P.; Boyd, P. W. D.; Burrell, A. K.; Robinson, W. T.; Taylor, M. J. *Inorg. Chem.* **1990**, *29*, 3593.
(14) (a) Møller, C.; Plesset, M. S. *Phys. Rev.* **1934**, *46*, 618. (b) Binkley, J. S.; Pople, J. A. *Int. J. Quantum Chem.* **1975**, *9S*, 229.
(15) Hehre, W. J.; Ditchfield, R.; Pople, J. A. *J. Chem. Phys.* **1972**, *56*, 2257.
(16) (a) Jonas, V.; Frenking, G.; Reetz, M. T. *J. Comput. Chem.* **1992**, *13*, 919. (b) Veldkamp, A.; Frenking, G. *Chem. Ber.* **1993**, *126*, 1325. (c) Möllmann, J.; Frenking, G.; Dötz, K.-H. *J. Am. Chem. Soc.*, submitted for publication.
(17) Pople, J. A.; Head-Gordon, M.; Raghavachari, K. *J. Chem. Phys.* **1987**, *87*, 5968.
(18) Ehlers, A. W.; Böhme, M.; Dapprich, S.; Gobbi, A.; Höllwarth, A.; Jonas, V.; Köhler, K. F.; Stegmann, R.; Veldkamp, A.; Frenking, G. *Chem. Phys. Lett.* **1993**, *208*, 111.
(19) *Gaussian 92*, Revision A.; Frisch, M. J., Trucks, G. W., Head-Gordon, M., Gill, P. M. W., Wong, M. W., Foresman, J. B., Schlegel, H. B., Raghavachari, K., Robb, M. A., Binkley, J. S., Gonzalez, C., Martin, R., Fox, D. J., DeFrees, D. J., Baker, J., Stewart, J. J. P., Pople, J. A., Eds.; Gaussian Inc.: Pittsburgh, PA, 1992.
(20) Biegler-König, F. W.; Bader, R. F. W.; Ting-Hua, T. *J. Comput. Chem.* **1982**, *3*, 317.

Table II. Theoretically Predicted (MP2/I) and Experimentally Observed Vibrational Frequencies (cm^{-1}) [Calculated Infrared Intensities (km/mol) in Parentheses]

$AgCO^+$ (1)			$Ag(CO)_2^+$ (2)			$Ag(CO)_3^+$ (3)	
symm	calc	exp[a]	symm	calc	exp[b]	symm	calc
Σ^+	201 (1.7)		Π_u	47 (0.0)		E′	18 (0.0)
Π	207 (0.1)		Σ_g^+	209 (0.0)		A_2''	40 (0.0)
Σ^+	2177 (4.4)	2204	Π_g	230 (0.0)		A_2'	168 (0.0)
			Π_u	260 (0.0)		E′	180 (0.7)
			Σ_u^+	281 (0.0)		E″	194 (0.0)
			Σ_g^+	2180 (0.0	2203	A_1'	197 (0.0)
			Σ_u^+	2180 (29.7)	2198	A_2''	224 (0.2)
						E′	235 (0.5)
						A_1'	2165 (0.0)
						E′	2166 (20.5)

$AuCO^+$ (4)			$Au(CO)_2^+$ (5)			$Au(CO)_3^+$ (6)	
symm	calc	exp[c]	symm	calc	exp[d]	symm	calc
Π	305 (0.0)	435	Π_u	66 (0.0)	105	E′	39 (2.4)
Σ^+	339 (11.6)	456	Π_g	312 (0.0)	312	A_2''	63 (0.5)
Σ^+	2175 (64.7)	2195	Σ_u^+	322 (0.0)	354	E′	191 (12.4)
			Σ_g^+	368 (0.0)	400	E″	251 (0.0)
			Π_u	396 (0.0)	406	A_2'	270 (0.0)
			Σ_u^+	2178 (0.0)	2217	A_1'	285 (0.0)
			Σ_g^+	2203 (29.7)	2254	A_2''	342 (6.4)
						E′	379 (1.0)
						E′	2155 (118.8)
						A_1'	2166 (0.0)

AgCN (7)			$Ag(CN)_2^-$ (8)		
symm	calcd	exp	symm	calc	exp[e]
Π	182 (6.3)		Π_u	71 (17.0)	107
Σ^+	364 (22.4)		Π_g	218 (0.0)	250
Σ^+	2094 (19.6)		Π_u	305 (5.3)	310
			Σ_g^+	325 (0.0)	360
			Σ_u^+	385 (35.0)	390
			Σ_u^+	2088 (1.0)	2140
			Σ_g^+	2089 (0.0)	2146

AuCN (9)		$Au(CN)_2^-$ (10)		
symm	calc	symm	calc	exp[f]
Π	279 (2.6)	Π_u	81 (13.9)	120
Σ^+	464 (8.6)	Π_g	284 (0.0)	302
Σ^+	2105 (18.8)	Σ_u^+	405 (20.7)	390
		Π_u	405 (0.1)	426
		Σ_g^+	426 (0.0)	440
		Σ_u^+	2094 (1.7)	2142
		Σ_g^+	2106 (0.0)	2162

CO			CN^-		
symm	calc	exp	symm	calc	exp
Σ^+	2118 (25.9)	2143	Σ^+	1997 (0.1)	2076

[a] Reference 3. [b] Reference 4. [c] Reference 23e. [d] Reference 5. [e] Reference 35. [f] Reference 31a,b. [g] Reference 79. [h] Reference 36.

The calculated Ag–C bond length in $AgCO^+$ (1) (2.329 Å) is slightly longer than that previously predicted (2.293 Å).[11] The experimentally reported Ag–C distance in $[Ag(CO)][B(OTeF_5)_4]$ measured by X-ray diffraction analysis[3] is significantly shorter (2.10 Å) than that calculated. However, the silver atom in $[Ag(CO)][B(OTeF_5)_4]$ is tricoordinated rather than monocoordinated. As shown below, a higher coordination of Ag(I) leads to a *shorter* Ag–C distance in $Ag(CO)X^+$ complexes. It follows that the discrepancy between theory and experiment for the Ag–C bond length in 1 is not caused by an error of either method, but by the molecular structure of $[Ag(CO)][B(OTeF_5)_4]$. The C–O distance in 1 is calculated as shorter (1.142 Å) than that of free CO (1.152 Å, Table I). This is in agreement with the experimental finding[3] that the carbonyl group in $[Ag(CO)][B(OTeF_5)_4]$ has a shorter bond length (1.077 Å) than CO (1.128 Å).[7a] The C–O stretching frequency in 1 is predicted at 2177 cm^{-1}, which is 59 cm^{-1} higher than in free CO (2118 cm^{-1}, Table II). The experimentally observed[3] frequency shift for ν_{CO} in $[Ag(CO)][B(OTeF_5)_4]$ is 61 cm^{-1} (Table II). The calculated Ag^+–CO dissociation energy D_e for 1 at QCISD(T)/II is 21.2 kcal/mol (Table III). A previous theoretical study predicted $D_e(1)$ = 19.2 kcal/mol.[11] There is no experimental value for the Ag^+–CO bond strength available.

The optimized structure of $Ag(CO)_2^+$ (2) has a linear geometry with Ag–C bond lengths which are *shorter* (2.216 Å, Table I) than that in 1. This is in contrast to most other second-row transition metal carbonyl ions $M(CO)_n^+$, which have longer M–C bond lengths for n = 2 than for n = 1.[11] The calculated Ag–C bond distance for 2 is in good agreement with a previous theoretical study[11] (2.226 Å) and with experimental data obtained from X-ray diffraction for $[Ag(CO)_2][B(OTeF_5)_4]$ showing values for r_{Ag-C} = 2.06–2.20 Å.[4] Table I shows that the correlation contributions to the calculated Ag–C bond lengths are

Table III. Calculated Reaction Energies (kcal/mol) Using Geometries Optimized at MP2/I for the Reactions

$$M^+ + CO \rightarrow M(CO)^+ \quad (I)$$

$$M(CO)^+ + CO \rightarrow M(CO)_2^+ \quad (II)$$

$$M(CO)_2^+ + CO \rightarrow M(CO)_3^+ \quad (III)$$

$$M^+ + CN^- \rightarrow M(CN) \quad (IV)$$

$$M(CN) + CN^- \rightarrow M(CN)_2^- \quad (V)$$

	I		II		III		IV		V	
	Ag	Au	Ag	Au	Ag	Au	Ag	Au	Ag	Au
MP2/1	−21.2	−39.5	−25.5	−48.5	−12.4	−8.5	−175.2	−217.1	−95.0	−116.0
MP3/1	−17.9	−33.5	−20.7	−42.8			−170.0	−210.5	−89.9	−111.2
MP4/1	−19.5	−36.5	−21.6	−45.3			−172.8	−214.4	−93.1	−113.3
QCISD/1	−19.2	−36.5	−22.8	−44.3			−173.0	−215.2	−92.2	−111.6
QCISD(T)/1	−19.8	−38.2	−23.6	−45.6			−174.7	−218.1	−93.2	−112.8
MP2/II	−23.0	−51.1	−29.5	−56.6			−181.0	−234.5	−100.4	−120.8
MP3/II	−18.8	−38.5	−22.8	−45.5			−173.4	−217.5	−92.3	−111.5
MP4/II	−20.4	−42.7	−25.6	−49.0			−176.3	−223.9	−95.8	−114.1
QCISD/II	−20.1	−42.3	−25.0	−47.3			−176.6	−224.2	−94.4	−111.6
QCISD(T)/II	−21.2	−45.1	−26.6	−49.5			−179.3	−228.5	−96.7	−114.0

important. The Ag–C distances for **1** and **2** are ~0.2 Å longer at the Hartree–Fock level than at MP2/I. The calculated C–O lengths for **2** are the same (1.143 Å) as for **1**, i.e. r_{CO} is predicted to be shorter than in free CO. The experimentally observed C–O distances for $[Ag(CO)_2][B(OTeF_5)_4]$ (1.07–1.09 Å)[4] are comparable to the bond length in $[Ag(CO)][B(OTeF_5)_4]$ (1.077 Å).[3] The asymmetric stretching frequency ν_{CO} in **2** is calculated as 2180 cm^{-1}, 62 cm^{-1} higher than that of CO (Table II). The experimental values for the IR active band ν_{CO}(asymm) in $Ag(CO)_2^+$ with different counterions[3] are 2198–2207 cm^{-1}, which is a shift of 55–64 cm^{-1} toward higher wavenumbers than those of CO.[7a] The calculated dissociation energy $D_e(AgCO^+–CO)$ (26.6 kcal/mol, Table III) is higher than $D_e(Ag^+–CO)$ (21.2 kcal/mol). Thus, the Ag(I) ion in **2** is bound with a total binding energy of 47.8 kcal/mol, but in **1** the Ag^+–CO binding energy is only 21.2 kcal/mol. The X-ray structure analysis of $[Ag(CO)_2][B(OTeF_5)_4]$ shows a nearly linear $Ag(CO)_2^+$ unit which is only weakly bonded to two or more $B(OTeF_5)_4^-$ anions.[4] In contrast to this the X-ray structure analysis of $[Ag(CO)][B(OTeF_5)_4]$ exhibits a tricoordinated Ag(I) atom with two short Ag–$OTeF_5$ distances.[3] It seems that only the additional coordination of the $AgCO^+$ cation by the $OTeF_5$ ligands allows the isolation of the monocarbonyl complex.

Is it possible to isolate a silver tricarbonyl ion? Because the solid state structure of $[Ag(CO)][B(OTeF_5)_4]$ shows a tricoordinated Ag(I) atom,[3] the synthesis of salt compounds of $Ag(CO)_3^+$ (**3**) seems possible. Table I shows that the optimized Ag–C bonds in **3** are rather long (2.322 Å), nearly as long as that in **1** (2.329 Å). But the dissociation energy for loss of one CO is much lower for **3** (12.4 kcal/mol at MP2/I) than for **1** and **2** (Table III). The lowest lying vibrational frequency of **3** is only 18 cm^{-1} (Table II). It follows that $Ag(CO)_3^+$ is only very weakly bound, probably too weak to be isolated as a salt.

The theoretically predicted Au–C distance in $AuCO^+$ (**4**) is 1.975 Å (Table I), which is significantly shorter than the Ag–C distance in **1** (2.329 Å). Because the ionic radius[21] of Au(I) is only slightly smaller (0.62 Å) than Ag(I) (0.68 Å), the short Au–C distance indicates a stronger bond for **4** than for **1**. The calculated dissociation energy $D_e(Au^+–CO)$ for **4** is 45.1 kcal/mol, which is more than twice what is calculated for **1** (21.2 kcal/mol, Table III). Thus, $AuCO^+$ is bound much stronger than $AgCO^+$. The theoretically predicted Au–C distance for **1** is slightly longer than the experimentally observed Au–C bond length in Au(CO)Cl (1.93 Å).[22] The calculated stretching frequency ν_{CO} for **1** (2175 cm^{-1}) is 57 cm^{-1} higher than that for CO. The experimentally observed values for ν_{CO} of Au(CO)X with X = Br, Cl, SO_3F are 11–53 cm^{-1} higher than that for CO.[23] This indicates negligible π back-donation in **4** like in **1**, although the Au–C bond in **4** is much shorter than the Ag–C bond in **1**.

The theoretically predicted Au–C distance in $Au(CO)_2^+$ (**5**) is 2.009 Å, which is slightly longer than that in **4**. The correlation contributions to the calculated Au–C distances in **4** and **5** are large, and the optimized bond lengths are significantly shorter at MP2/I than at HF/I (Table I). An X-ray structure analysis of $[Au(CO)_2][Sb_2F_{11}]$ is not available, but from a comparison of the force constants using the experimental vibrational spectrum of $[Au(CO)_2][Sb_2F_{11}]$ with related gold compounds an estimate of 2.05 Å for $r_{Au–C}$ was made.[5] This is in reasonable agreement with our theoretical value of 2.009 Å. The calculated bond strength $D_e(AuCO^+–CO)$ is 49.5 kcal/mol (Table III), slightly higher than the Au–CO bond strength in **4**. The gold(I) carbonyls are theoretically predicted to be bound much stronger than the silver(I) carbonyls.

Table II shows the calculated and experimental fundamentals of the vibrational spectrum of **5**. The earlier assignment of the fundamental vibrations[23e,24] of $Au(CO)_2^+$ was recently corrected.[5] Our calculated wavenumbers of the fundamentals are in agreement with the assignment made by Willner et al.[5] shown in Table II. The symmetric and asymmetric CO stretching frequencies are calculated at 2203 and 2178 cm^{-1}, respectively. These are 85 and 60 cm^{-1} higher than that of CO, respectively. The experi-

(21) Liao, M. S.; Schwarz, W. H. E. *Angew. Chem.*, in press.

(22) Jones, P. G. *Z. Naturforsch.* **1982**, *37B*, 823.

(23) (a) Belli Dell'Amico, D.; Calderazzo, F.; Robino, P.; Serge, A. *Gazz. Chim. Ital.* **1991**, *121*, 51; *J. Chem. Soc., Dalton Trans.* **1991**, 3017. (b) Belli Dell'Amico, D.; Calderazzo, F.; Dell'Amico G. *Gazz. Chim. Ital.* **1977**, *107*, 101. (c) Calderazzo, F. *Pure Appl. Chem.* **1978**, *50*, 49. (d) Browning, J.; Goggin, P. L.; Goodfellow, R. J.; Norton, M. J.; Rattray, A. J. M.; Taylor, B. F.; Mink, J. *J. Chem. Soc., Dalton Trans.* **1977**, 2061. (e) Willner, H.; Aubke, F. *Inorg. Chem.* **1990**, *29*, 2195.

(24) Adelhelm, M.; Bacher, W.; Höhn, E. G.; Jacob, E. *Chem. Ber.* **1991**, *124*, 1559.

mentally observed frequency shifts[5] toward higher wavenumbers are 111 and 74 cm^{-1}. The large frequency shifts indicate that there should be no π back-donation by the metal atom into the π^* orbitals of the carbonyl ligands in **5**.

The gold tricarbonyl ion **6** is predicted with a long (2.096 Å, Table I) and weak ($D_e(Au(CO)_2^+-CO)$ = 8.5 kcal/mol at MP2/I, Table III) Au–C bond. The lowest lying fundamental has a wavenumber of only 39 cm^{-1} (Table II). Like the silver tricarbonyl ion **3**, the gold ion **6** is only a weakly bonded species, probably too weakly bound to be isolated as a salt. It might, however, play a role as an intermediate in substitution reactions.

The cyano ligand CN^- is a stronger donor than CO, and the optimized geometry for AgCN (**7**) has a significantly shorter Ag–C bond (2.087 Å) than **1** (Table I). The C–N bond in **7** is calculated shorter (1.188 Å) than that for isolated CN^- (1.202 Å), which indicates that CN^- is dominantly a σ donor in **7**, like CO in **1**. The theoretically predicted energy calculated for the dissociation of **7** into $Ag^+ + CN^-$ (reaction IV, Table III) may be used to estimate the Ag–C bond strength of AgCN. The experimentally observed first ionization energy of Ag is 7.576 eV,[25] and the electron affinity of CN is 3.82 eV.[26] Combining these data with the calculated reaction energy for reaction IV gives a theoretically predicted bond energy of D_e = 92.7 kcal/mol for the Ag–C bond of **7**. This is substantially higher than the Ag–C bond energy of **1** (21.2 kcal/mol) (Table III).

The calculated vibrational spectrum of **7** shows a stretching frequency of 2094 cm^{-1} for the C–N stretching mode, 97 cm^{-1} higher than that of isolated CN^- (Table II). AgCN has a linear polymeric structure. There are no experimental values for isolated **7** to compare with the theoretical results. Experimental results are available, however, for $Ag(CN)_2^-$ (**8**). The Ag–CN bonds in **8** are calculated with nearly the same interatomic distance (2.090 Å) as that in **7** (Table I). This is different from the Ag–CO^+ bonds in **2**, which are significantly shorter than that in **1** (Table I). The analysis of X-ray diffraction measurements of solid **8** with different counterions shows[27,28] values for the Ag–C bond length between 2.01 and 2.07 Å, in good agreement with the calculated value. Theory and experiment agree that the C–N distances in **8** are shorter than that of isolated CN^-. The calculated vibrational spectrum of **8** (Table II) predicts a frequency shift of 91 and 92 cm^{-1} toward higher wavenumbers for the symmetric and asymmetric vibration of the C–N stretching mode. The experimentally observed[27] shifts are 70 and 64 cm^{-1}. The calculated bond energy of the $Ag(CN)–CN^-$ bond in **8** (96.7 kcal/mol) is much higher than the $AgCO^+–CO$ bond energy in **2** (26.6 kcal/mol, Table III). It is also slightly higher than the calculated dissociation energy D_e(Ag–CN) = 92.7 kcal/mol.

AuCN (**9**) is theoretically predicted with a rather short Au–C bond (1.929 Å), shorter than the Au–C bond in **4** (Table I). Combining the calculated reaction energy for dissociation of **4** into $Au^+ + CN^-$ (228.5 kcal/mol, reaction IV, Table III) with the experimentally reported ionization energy of Au (9.225 eV[25]) and the electron affinity of CN (3.82 eV[26]) gives a theoretically predicted bond energy D_e(Au–C) for **9** of 103.9 kcal/mol. Thus, AuCN has a stronger M–CN bond than AgCN. The calculated C–N bond of **9** is shorter and the C–N stretching fundamental has a higher frequency than CN^- (Tables I and II). Experimental values are not available for isolated AuCN but for $Au(CN)_2^-$ (**10**). The calculated Au–C distances for **10** (2.005 Å) are in good agreement with the results of an X-ray structure analysis,[29] which give values of 1.91–2.06 Å. Earlier values of 2.12 ± 0.14 Å should be reinvestigated.[30] The geometries of **9** and **10** have been optimized in previous theoretical studies[13] at the Hartree–Fock level. The Au–C bonds were predicted as 2.026 Å for **9** and 2.075 Å for **10**.[13] The results in Table I show that correlation energy has a strong effect upon the calculated Au–C bond lengths and that the Au–C interatomic distance is significantly shorter and in better agreement with experiment than the bond length calculated at the Hartree–Fock level. The C–N distances in **10** are predicted to be shorter (1.189 Å) than that of CN^-. The experimental values[29] for r_{CN} of **10** are 1.12–1.18 Å.

The calculated vibrational spectrum of **10** shown in Table III is also in good agreement with the experimentally observed spectra.[28] The C–N stretching mode is predicted to be 109 cm^{-1} (Σ_g^+) and 97 cm^{-1} (Σ_u^+) higher than that of CN^- (Table III). The experimentally observed shifts[31] toward higher wavenumbers are 86 cm^{-1} (Σ_g^+) and 66 cm^{-1} (Σ_u^+). The $Au(CN)–CN^-$ bond energy is calculated to be very high (D_e = 114.0 kcal/mol), higher than the $Ag(CN)–CN^-$ bond energy (96.7 kcal/mol) and much higher than the dissociation energy for the $AuCO^+–CO$ bond in **5** (49.5 kcal/mol, Table III). It is also higher than the Au–CN bond energy in **9** (103.9 kcal/mol). Previous theoretical studies carried out at the Hartree–Fock level give a dissociation energy D_e(Au–CN) for **9** of only 58.1 kcal/mol, and for the $Au(CN)–CN^-$ bond of **10** they give D_e = 84.2 kcal/mol.[13] Since correlation contributions are included in our calculations, we think that our results are more reliable.

In order to convert the calculated D_e values for loss of CO or CN^- to experimental binding energies E_0[298], we must correct for zero-point vibration ZPE and vibrational excitation VE(298). By assuming that the system is an ideal gas, we may correct classically for rotational and translational effects ΔRT. This leads to a contribution of $^5/_2$ RT (**1**, **4**, **7**, **9**), $^7/_2$ RT (**2**, **5**, **8**, **10**), and 3 RT (**3**, **6**). The results shown in Table IV clearly indicate that (i) the cyano compounds are bound much stronger than the carbonyls, (ii) the gold compounds are bound stronger than the silver compounds (with exception of the weakly bound tricarbonyls), (iii) the dissociation energy of the first carbonyl and cyano ligand in $M(CO)_2^+$ and $M(CN)_2^-$ is higher than the dissociation energies of MCO^+ and MCN, respectively, and (iv) the bond energy of the third carbonyl ligand in **3** and **6** is very low.

We investigated the electronic structure of **1**–**10** using the topological analysis of the electron density distribu-

(25) Moore, C. E. *Analyses of Optical Spectra*; NSRDS-NBS 34; Office of Standard Reference Data, National Bureau of Standards: Washington, DC, 1971.
(26) Berkowitz, J.; Chupka, W. A.; Walter, T. A. *J. Chem. Phys.* **1969**, *50*, 1497.
(27) Jones, L. H. *J. Chem. Phys.* **1957**, *26*, 1578.
(28) (a) Range, K.-J.; Kühnel, S.; Zabel, M. *Acta Crystallogr.* **1989**, *C45*, 1419. (b) Range, K.-J.; Zabel, M.; Meyer, H.; Fischer, H. *Z. Naturforsch.* **1985**, *40B*, 1618. (c) Zabel, M.; Kühnel, S.; Range, K.-J. *Acta Crystallogr.* **1989**, *C45*, 1619. (d) Kappenstein, C.; Ouali, A.; Guerin, M.; Cernak, J.; Chomic, J. *Inorg. Chim. Acta* **1988**, *147*, 189.
(29) Schübert, R. J.; Range, K.-J. *Z. Naturforsch.* **1990**, *45B*, 629.
(30) (a) Rosenzweig, A.; Cromer, D. T. *Acta Crystallogr.* **1959**, *B12*, 705. (b) Staritzky, E. *Anal. Chem.* **1956**, *28*, 419.
(31) (a) Chadwick, B. M.; Frankiss, S. G. *J. Mol. Struct.* **1976**, *31*, 1. (b) Jones, L. H. *J. Chem. Phys.* **1957**, *27*, 468.

Table IV. Dissociation Energies for the Dissociation of One C–X Fragment

	1	2	3	4	5	6	7	8	9	10
D_e[a]	21.2	26.6	12.4	45.1	49.5	8.5	92.7	96.7	103.9	114.0
ZPE[b]	−1.0	−1.5	−0.5	−1.5	−2.5	−0.6	−1.1	−1.8	−1.6	−2.0
VE(298)[c]	−2.0	−3.4	−2.4	−2.2	−3.6	−2.4	−2.1	−3.4	−2.3	−3.6
ΔRT[d]	+1.5	+2.1	+1.8	+1.5	+2.1	+1.8	+1.5	+2.1	+1.5	+2.1
D_0^{298}	19.7	23.8	11.3	42.9	45.5	7.3	91.0	93.6	101.5	110.5

[a] Calculated at QCISD(T)/II//MP2/I. For **3** and **6** the results are calculated at MP2/II//MP2/I. The dissociation energies for **7** and **9** are given for the reaction MCN → M + CN using the results from Table III and the experimental ionization energy of M and electron affinity of CN. [b] Zero point vibration correction. [c] Vibrational excitation correction. [d] Rotational and translational correction (see text).

Table V. Results of the Topological Analysis of the Wave Function Calculated at MP2/I[a]

	$\nabla^2\rho_b$	H_b	ρ_b	r_b(F)
CO	31.8071	−4.9640	3.0340	0.328
		$AgCO^+$ (**1**)		
Ag–C	5.2847	−0.0587	0.3819	0.516
C–O	32.6650	−5.2110	3.1136	0.331
		$Ag(CO)_2^+$ (**2**)		
Ag–C	6.3017	−0.1188	0.4940	0.518
C–O	32.1806	−5.2272	3.1167	0.331
		$Ag(CO)_3^+$ (**3**)		
Ag–C	5.4438	−0.0607	0.3853	0.517
C–O	31.9975	−5.1975	3.1076	0.330
		$AuCO^+$ (**4**)		
Au–C	9.4368	−0.3772	0.9380	0.542
C–O	31.5613	−5.2704	3.1170	0.332
		$Au(CO)_2^+$ (**5**)		
Au–C	9.5356	−0.3097	0.8604	0.532
C–O	31.3155	−5.2866	3.1265	0.355
		$Au(CO)_3^+$ (**6**)		
Au–C	5.1425	−0.0938	0.4400	0.526
C–O	32.0673	−5.2258	3.1143	0.331
CN^-	2.5279	−5.1637	2.9173	0.332
		AgCN (**7**)		
Ag–C	6.4944	−0.2362	0.6714	0.531
C–N	4.3690	−5.3034	2.9618	0.336
		$Ag(CN)_2^-$ (**8**)		
Ag–C	6.6655	−0.2402	0.6762	0.524
C–N	2.2218	−5.3330	2.9760	0.336
		AuCN (**9**)		
Au–C	5.9715	−0.5203	1.0642	0.553
C–N	5.0293	−5.2467	2.9416	0.338
		$Au(CN)_2^-$ (**10**)		
Au–C	7.9789	−0.3536	0.8948	0.534
C–N	1.4387	−5.3405	2.9766	0.338

[a] Laplacian concentration $\nabla^2\rho_b$ (e Å^{-5}), energy density H_b (hartree Å^{-3}), and electron density ρ_b (e Å^{-3}) at the bond critical point. r_b(F) gives the position of the bond critical point r_b for the bond A–B calculated by the ratio $r_b(F) = r(A - r_b)/r(A–B)$

tion[10] and the natural bond orbital method[9] in order to investigate the peculiar M–CO bonding. Previous studies[11,32] suggest that the bonding in transition metal carbonyl ions MCO^+ and $M(CO)_2^+$ is dominantly electrostatic. However, a significant amount of covalent Ag–C bonding in $AgCO^+$ and $Ag(CO)_2^+$ involving the silver 5s orbital is indicated by the large $J(^{109}Ag^{13}C)$ coupling constant observed for **1** and **2**.[4] Another question concerns the nature of the covalent contribution to the M–C bonds in **1–10**, i.e. the participation of metal d(σ) and p(σ) orbitals in the σ bonds and the extent of π back-donation, which is assumed to be very small.[3–5]

Figure 1 shows the Laplacian distribution for **1–10** and for CO and CN^-. Table V shows the results of the topological analysis of the wave function. The most important results of the NBO analysis are listed in Table VI.

Visual inspection of the contour line diagrams shown in Figure 1 demonstrates that the electronic structures of the CO and CN^- ligands change very little upon complexation with the metal atoms. This is also shown by the calculated values for the topological analysis of the wave function listed in Table V. The position of the bond critical point r_b for the CO and CN bonds is shifted a little bit away from C toward O (N) in **1–10** relative to CO and CN^-. The energy densities at the bond critical point H_b for the CO and CN bonds are more negative in **1–10** than in CO and CN, which indicates that the ligand bonds become slightly more covalent upon complexation.[33]

What about the metal–ligand bonds in **1–10**? The contour line diagrams displayed in Figure 1 show a nearly isotropical Laplacian distribution for the metal atoms. The calculated charge distribution gives a partial charge of +0.97 for Ag in **1**, which means that transfer of electronic charge from CO to Ag^+ is negligible. The major interaction between Ag^+ and CO in **1** appears to be the polarization of the charge distribution in CO by Ag^+, which shows the largest change compared with the isolated fragments (Table VI). The NBO analysis predicts that the 5s(Ag) orbital is populated by only 0.05 e. This indicates weak electron donation by the σ(CO) lone pair MO. The breakdown of the electronic structure into bond orbitals shows no Ag–C bond orbital, but rather a carbon lone-pair MO. Back-donation is nearly zero, and the π^*(CO) population is 0.01 e (Table VI). This is very similar to the results of a Mulliken population analysis reported for **1**.[11]

Further support for a dominantly electrostatic Ag–C bond in **1** comes from the energy density at the bond critical point H_b. It has been shown that the value of H_b is a very sensitive probe for the type of bonding.[33] Covalent bonds have negative values typically between −1 and −4, whereas closed shell interactions have $H_b \sim 0$.[33] Table V shows that H_b for the Ag–C bond of **1** is only −0.06. Thus, all theoretical data suggest that the Ag–C bond in **1** should be considered as electrostatic. This seems to be in disagreement with the $J(^{109}Ag^{13}C)$ coupling constant measured for $[Ag(CO)][B(OTeF_5)_4]$.[4] As discussed before, the Ag atom in this complex is tricoordinated and not monocoordinated, and the observed Ag–CO distance is much shorter than that calculated for **1**.[3] Although $[Ag(CO)][B(OTeF_5)_4]$ is formally a silver monocarbonyl complex, the structural features cannot be compared with

(32) Mavridis, A.; Harrison, J. F.; Allison, J. *J. Am. Chem. Soc.* **1989**, *111*, 2482.

(33) Cremer, D.; Kraka, E. *Angew. Chem.* **1984**, *96*, 612; *Angew. Chem., Int. Ed. Engl.* **1984**, *23*, 627.

(34) Experimental value for NaCN: Fontaine, D. *C. R. Acad. Sci.* **1975**, *281B*, 443.

(35) Jones, L. H.; Penneman, R. A. *J. Chem. Phys.* **1954**, *22*, 965.

(36) Value measured for KCN: Siebert, H. *Anwendung der Schwingungsspektroskopie in der anorganischen Chemie*; Springer: Heidelberg, 1966.

Table VI. Results of the NBO Analysis

	population[a]				M–C bond[a,b]				charges		
	*n*s	(*n* – 1)d	*n*p	π*(C–X)	% M	% *n*s(M)	% *n*p(M)	% (*n* – 1)d(M)	q_M	q_C	q_x
$Ag(CO)^+$ (**1**)	0.05	9.98	<0.01	<0.01	no M–C bond				+0.97	+0.49	–0.46
$Ag(CO)_2^+$ (**2**)	0.27	9.92	<0.01	<0.01	5.8	96.6	0.5	2.8	+0.82	+0.54	–0.45
$Ag(CO)_3^+$ (**3**)	0.17	9.97	0.01	<0.01	no M–C bond				+0.85	+0.53	–0.48
$Au(CO)^+$ (**4**)	0.28	9.82	<0.01	0.08	9.7	93.4	0.8	5.9	+0.90	+0.51	–0.40
$Au(CO)_2^+$ (**5**)	0.70	9.69	<0.01	0.05	14.8	87.3	0.2	12.4	+0.61	+0.60	–0.41
$Au(CO)_3^+$ (**6**)	0.40	9.85	0.01	0.03	6.9	95.1	1.9	3.0	+0.78	+0.53	–0.44
Ag(CN) (**7**)	0.23	9.95	0.02	0.01	10.2	94.0	3.6	2.4	+0.80	–0.33	–0.48
$Ag(CN)_2^-$ (**8**)	0.59	9.84	0.02	0.02	13.2	91.2	1.0	7.8	+0.56	–0.19	–0.58
Au(CN) (**9**)	0.60	9.79	0.01	0.04	21.8	88.5	0.4	11.1	+0.60	–0.18	–0.43
$Au(CN)_2^-$ (**10**)	0.92	9.66	0.02	0.04	20.0	81.1	0.5	18.5	+0.41	–0.14	–0.56
CO										+0.60	–0.60
CN^-										–0.19	–0.81

[a] $n = 5$ for Ag, $n = 6$ for Au. [b] % M gives the contribution of the M–C bond orbital at atom M; % *n*s (M), % (*n* – 1)d(M), and % *n*p(M) give the hybridization of the M–C bond at M.

1. It will be very difficult to observe a truely monocoordinated complex of 1.

Unlike for 1, there is a distinct charge transfer in 2 from CO to Ag^+. The partial charge at Ag^+ is 0.82 (0.97 in 1), and the charge at C is 0.54 (0.49 in 1), while the charge at O is nearly the same in 2 (–0.45) as in 1 (–0.46). The NBO analysis attributes the charge transfer to a donation from CO nearly exclusively into the 5s(Ag) orbital, which is occupied by 0.27 e (Table VI). The Ag–C bond orbital calculated by the NBO partitioning scheme is localized to 94.2% at C and 5.8% at Ag. The latter part consists of 96.6% 5s(Ag) and 2.8% d(Ag). This is in agreement with the experimentally observed $J(^{109}Ag^{13}C)$ coupling constant in $[Ag(CO)_2][B(OTeF_5)_4]$, which indicates covalent contributions to the Ag–C bond.[4] A partly covalent character is also suggested by the H_b value for the Ag–C bond in 2 (–0.12, Table V). The π* back-donation into the π*(CO) orbital is vanishingly small (<0.01 e, Table VI), which is in agreement with the interpretation based upon the CO frequency shift.[4] The Ag–C bond in 3 is dominantly electrostatic in origin, as revealed by the low occupancy of the 5s orbital (0.17 e) and the H_b value (–0.06). The NBO analysis gives no Ag–C bond orbital for 3.

The NBO analysis of $AuCO^+$ indicates a charge donation from CO to the metal higher than that in $AgCO^+$ (Table VI). The partial charge at Au in 4 is +0.90. The breakdown of the orbital contributions shows that the 6s(Au) orbital in 4 is occupied by 0.28 e, nearly the same as the 5s(Ag) occupancy in 2. The slightly smaller 5d(Au) occupation could mean that the 5d electrons are not as corelike as the 4d(Ag) electrons in 1 and 2. A contribution of 5.9% of the dσ(Au) orbitals to the Au–C bond, which is localized to 90.3% at C, is calculated for 4 by the NBO analysis (Table VI). The π back-donation into the CO π* orbital is 0.08 e, the highest of the investigated complexes, but still rather small. The energy density at the bond critical point H_b suggests that the Au–C bond in 4 has a partly covalent character ($H_b = -0.38$) which is clearly higher than the covalent character of the Ag–C bond in 2 ($H_b = -0.12$, Table V). A slightly smaller covalent contribution is analyzed for the Au–C bond in 5 ($H_b = -0.310$, Table V). The positive charge at Au in 5 is only 0.61. It follows that in 5 a significant amount of electronic charge is transferred from CO to Au^+. The occupancy of the 6s(Au) orbital is quite high (0.70 e, Table VI). The Au–C bond orbital of 5 calculated by the NBO method is localized to 14.8% at Au and consists of 87.3% s(Au) and 12.4% dσ(Au). There is very little π* back-donation into the π*(CO) orbital of 5, as shown by the calculated occupancy (0.05 e, Table VI).

Although the NBO analysis gives a Au–C bond orbital for 6, the bond is localized to 93.1% at C. The occupancy of the 6s(Au) orbital is significantly lower in 6 than in 5. The calculated H_b value for the Au–C bond in 6 (–0.09) shows that this bond has much less covalent character than the bonds in 4 and 5. This is a very interesting result: Although the addition of one CO to 5 gives an energy minimum structure 6 which has a higher (total) bond energy, the character of the Au–C bond in 6 is very different from that of 5. The Au–C bonds in 6 are almost purely electrostatic ($H_b = -0.09$), while the Au–C bonds in 5 have significant covalent contributions ($H_b = -0.31$). A similar result is found for 2 and 3 (Table V). Thus, the addition of a third CO ligand to 2 and 5 changes the nature of the metal–ligand bonds significantly!

A comparison of the electronic structures of the cyano complexes 7–10 with the corresponding carbonyl complexes 1, 2, 4, and 5 may be given as follows. As mentioned above, we discuss the cyano complexes as products of M^+ and CN^-. Then, the charge transfer from CN^- to M^+ in 7–10 is larger than from CO to M^+, as expected. The differences are not very large, though. The metal atoms carry always a positive charge, also in the anionic complexes 8 and 10. The NBO analysis calculates higher occupied 5s(Ag) and 6s(Au) orbitals in the cyano complexes than in the corresponding carbonyls (Table VI). The H_b values for the M–CN bonds are more negative than the corresponding M–CO bonds. It follows that the M–CN bonds of the cyano compounds 8–10 have larger covalent contributions than the M–CO bonds of 1–5. The NBO analysis shows that the M–CN bond orbitals have larger coefficients at M than the M–CO orbitals and slightly higher s–d(σ) mixing.

The analysis of the electronic structures of 1–10 may be summarized as follows. The carbonyl complexes 1–10 have M–CO bonds which should be considered as dominantly electrostatic with small but distinct covalent contributions in 2–10. The covalent contributions are larger in the gold complexes than in the corresponding silver molecules, and they are larger in the cyano complexes than in the metal carbonyls.

4. Summary

The optimized geometries of the silver and gold carbonyls and cyanides 1–10 have M–C bond lengths which are in good agreement with experimentally available

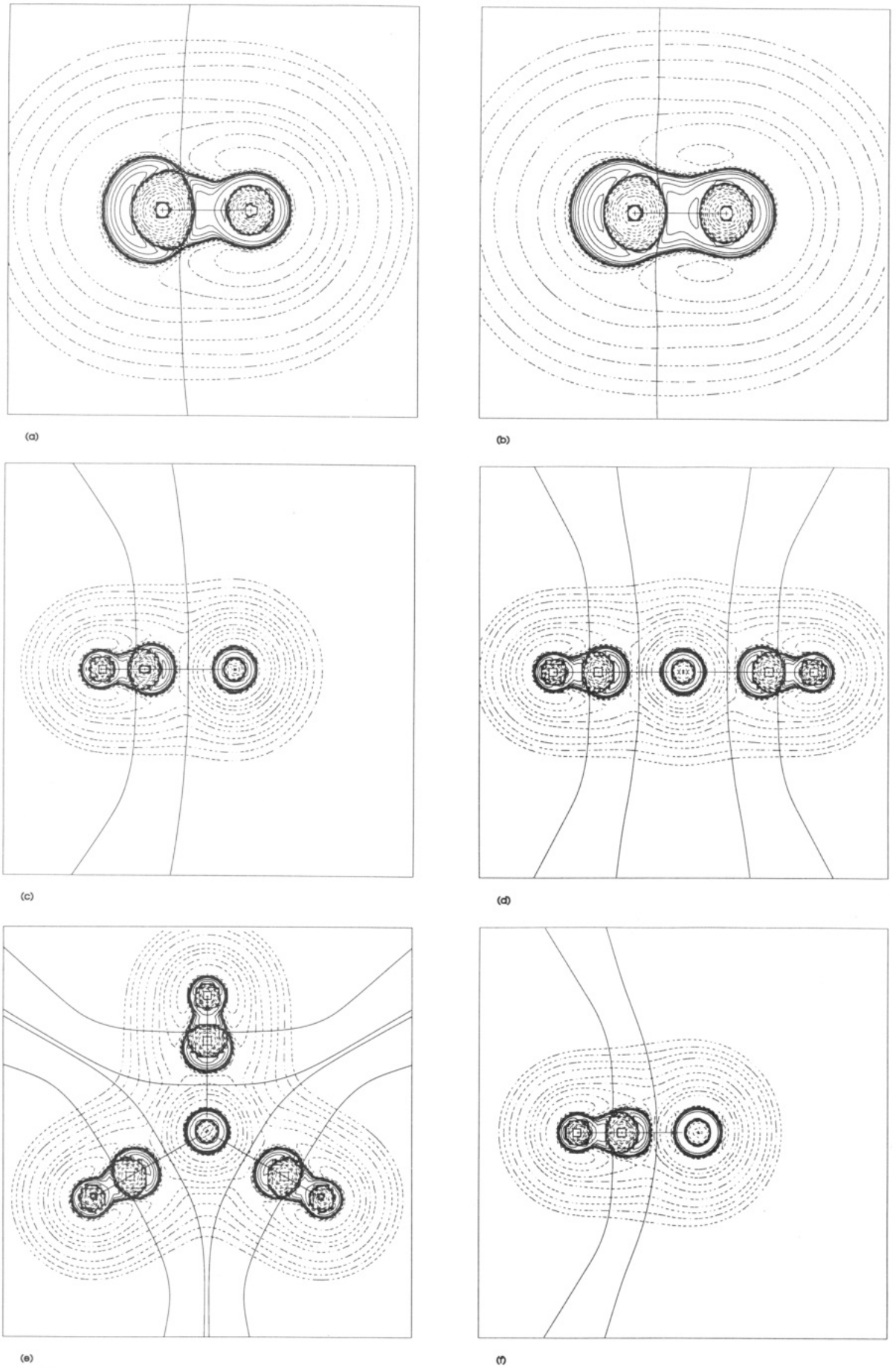

Figure 1. Contour line diagrams of the Laplacian distribution $\nabla^2\rho(\mathbf{r})$ of CO (a), CN^- (b), $AgCO^+$ (**1**) (c), $Ag(CO)_2^+$ (**2**) (d), $Ag(CO)_3^+$ (**3**) (e), $AuCO^+$ (**4**) (f), $Au(CO)_2^+$ (**5**) (g), $Au(CO)_3^+$ (**6**) (h), AgCN (**7**) (i), $Ag(CN)_2^-$ (**8**) (j), AuCN (**9**) (k), and $Au(CN)_2^-$ (**10**) (l). Dashed lines indicate charge depletion ($\nabla^2\rho(\mathbf{r}) > 0$); solid lines indicate charge concentration ($\nabla^2\rho(\mathbf{r}) < 0$). The solid

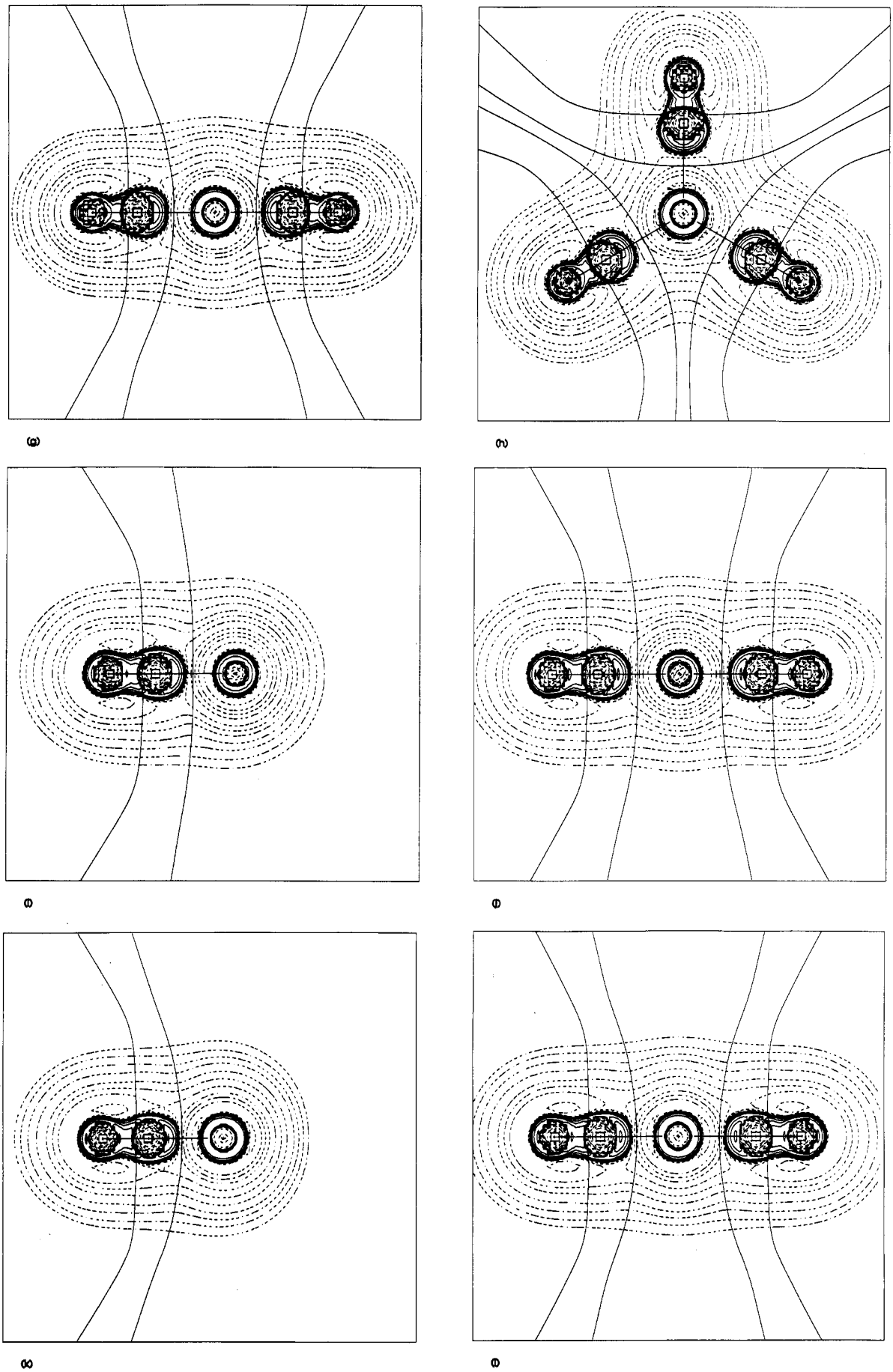

Figure 1 (continued).
lines connecting the atomic nuclei are the bond paths; the solid lines separating the atomic nuclei indicate the zero-flux surfaces in the molecular plane. The crossing points of the bond paths and zero-flux surfaces are the bond critical points $\mathbf{r}_b$.

results. The experimentally determined Ag–C distance in $[Ag(CO)][B(OTeF_5)_4]$, which is much shorter than that calculated for $AgCO^+$, is caused by the additional coordination of 1 by the anions. The theoretically predicted C–O and C–N stretching frequencies are shifted toward higher wavenumbers in the metal complexes **1–10**, which agrees with the experimentally observed vibrational spectra. The metal–ligand bond energies are much higher in the cyano compounds than in the carbonyls. The dissociation energy for loss of one CO is higher for the dicarbonyls than for the monocarbonyls, but much lower for the tricarbonyls. The theoretical data indicate that it will be difficult to isolate $Ag(CO)_3^+$ and $Au(CO)_3^+$ complexes and truly monocoordinated $AgCO^+$ and $AuCO^+$ complexes. The gold carbonyls $AuCO^+$ and $Au(CO)_2^+$ are bound significantly stronger than the silver carbonyls $AgCO^+$ and $Ag(CO)_2^+$. The metal–ligand bonds in **1–10** are dominantly electrostatic, but covalent contributions are analyzed for **2**, **7**, and **8** and particularly for **4**, **5**, **9**, and **10**. The nature of the metal–ligand bonds in **2** and **5** upon addition of another CO is found to change significantly. The M–C bonds in **3** and **6** are almost purely electrostatic.

Acknowledgment. This work has been supported by the Deutsche Forschungsgemeinschaft (SFB 260) and the Fonds der Chemischen Industrie. We acknowledge computer time by the computer center of the Hessischer Höchstleistungsrechner on the Siemens S400. Additional support was given by the computer companies Silicon Graphics and Convex.

OM930575N